NUCL SCI TECH (2021) 32:130
https://doi.org/10.1007/s41365-021-00967-y

Investigation of decay modes of superheavy nuclei

H. C. Manjunatha[1] · N. Sowmya[1] · P. S. Damodara Gupta[1] · K. N. Sridhar[2] · A. M. Nagaraja[1,3] · L. Seenappa[1] · S. Alfred Cecil Raj[3]

Received: 13 July 2021 / Revised: 28 August 2021 / Accepted: 31 August 2021 / Published online: 23 November 2021

Abstract A detailed investigation of different decay modes, namely alpha decay, beta decay, cluster decay, including heavy particle emission ($Z_c > 28$), and spontaneous fission, was carried out, leading to the identification of new cluster and beta-plus emitters in superheavy nuclei with $104 \leq Z \leq 126$. For the first time, we identified around 20 beta-plus emitters in superheavy nuclei. Heavy-particle radioactivity was observed in superheavy elements of atomic number in the range $116 \leq Z \leq 126$. $^{292-293}$Og were identified as ^{86}Kr emitters, and ^{298}122 and ^{300}122 were identified as ^{94}Zr emitters, whereas heavy-particle radioactivity from ^{91}Y was also observed in ^{299}123. Furthermore, the nuclei ^{300}124 and ^{306}126 exhibit ^{96}Mo radioactivity. The reported regions of beta-plus and heavy-particle radioactivity for superheavy nuclei are stronger than those for alpha decay. The identified decay modes for superheavy nuclei are presented in a chart. This study is intended to serve as a reference for identifying possible decay modes in the superheavy region.

Keywords Alpha decay · Beta decay · Heavy-particle radioactivity · Branching ratios

✉ H. C. Manjunatha
manjunathhc@rediffmail.com

[1] Department of Physics, Government College for Women, Kolar, Karnataka 563101, India

[2] Department of Physics, Government First Grade College, Kolar, Karnataka 563101, India

[3] Department of Physics, St. Joseph's College, Affiliated to Bharathidasan University, Tiruchirappalli, Tamil Nadu, India

1 Introduction

The most important unanswered questions in Nuclear Physics are to determine the heaviest superheavy nuclei that can exist, and to investigate whether very-long-lived superheavy nuclei exist in nature. The past ten years have been marked by remarkable progress in the science of superheavy elements and nuclei. The existence of superheavy nuclei above $Z = 103$ can be studied in terms of whether they can occur naturally or can be synthesized in the laboratory. There are no definitive conclusions regarding the existence of superheavy nuclei in nature. In contrast, such superheavy nuclei, with half-lives ranging between days to μs, can be synthesized using cold and hot fusion reactions. Cold fusion reactions involve either lead or bismuth as targets [1], whereas hot fusion reactions include ^{48}Ca beams on various actinide targets [2, 3]. Many theoretical predictions, such as microscopic–macroscopic [4] (single-particle potential) and self-consistent approaches, including nucleus–nucleus potential [5, 6], relativistic field models [7, 8], and multinucleon transfer reactions [9], provide information regarding the nucleus structure, shell closure location, and decay modes in heavy and superheavy nuclei.

The discovery of superheavy elements [10, 11] points to the island of stability. Boilley et al. [12] predicted the evaporation residue cross sections in superheavy elements and the influence of shell effects [13]. The entrance channel dynamics were studied using ^{48}Ca as a projectile and ^{208}Pb as target [14]. In 1966, two groups of researchers, namely Mayers and Swiatecki, and Viola and Seaborg [15], separately predicted the presence of heavy nuclei near the island of stability. Later, Sobiczewski et al. [16] predicted that the nucleus $Z = 114$ will be the center of the

island of stability, with neutron number $N = 184$. In 1955, Nilsson [17] proposed a shell model which includes deformation property of the nuclei. Bender et al. [18] used a Skyrme energy density functional model and studied the deformation properties of closed proton and neutron shells. The nuclear mass, radius, and spectroscopy far away from the valley of stability were experimentally analyzed earlier [19]. The investigation of isomers of the superheavy nucleus ^{254}No is a stepping stone toward the island of stability [20]. Previous researchers [21] analyzed the nuclear shell structure and discovered additional stability near magic nuclei. The present scenario is almost near the center of the presumed island of stability, but the final landing is yet to be completed, and the intriguing question is how these superheavy nuclei are still accessible.

The identification of superheavy nuclei is based on observations of decay chains. Superheavy element region $114 \leq Z \leq 118$ were observed owing to their consistent decay chains, which end in the isotopes of rutherfordium (Rf) and dubnium (Db). Spontaneous fission and α-decay are the dominant decay modes in superheavy nuclei and limit their stability. Furthermore, newly synthesized superheavy elements are primarily identified by their decay chains from unknown nuclei to known daughter nuclei by using the parent-and-daughter correlation.

The competition between different decay modes, such as ternary fission, spontaneous fission, cluster decay, proton decay, β-decay, and α-decay, in the heavy and superheavy region, has been extensively studied using various theoretical models, such as Coulomb and proximity potential models, modified generalized liquid drop models, effective liquid drop models, and temperature-dependent proximity potential models [22–33]. The possible decay modes in the superheavy nuclei $Z = 119$ and 120 are predicted in Ref. [34]. From Ref. [35], it is clearly observed that the isotopes of the superheavy nuclei $Z = 104$–112 have α−decay and spontaneous fission as dominant decay modes. However, only α-decay is dominant in the isotopes of superheavy nuclei $Z = 113$, 115–118. The isotopes of the superheavy nucleus $Z = 114$ have spontaneous fission as the dominant decay mode in the nucleus ^{284}Fl, α-decay is dominant in the nuclei $^{286-289}$Fl, and β^+ is dominant in the nucleus ^{290}Fl. Furthermore, the concept of heavy-particle radioactivity [36] in the superheavy region has important applications in the synthesis of superheavy nuclei. Despite the significant experimental and theoretical progress, there are many unanswered questions related to the decay modes of superheavy nuclei. Until now, only α-decay and spontaneous fission have been successfully observed in experiments.

Experimental results suggest a considerable increase in the lifetime of nuclei as they approach closed proton and neutron shells [37]. The lifetimes of most known superheavy nuclei are governed by the competition between α-decay and spontaneous fission. The existence of the island of stability has been confirmed experimentally in the previous decade [38]. Some theoretical studies reveal that superheavy elements with 114 and 164 protons are stable against fission as well as alpha and beta decay [39]. Various phenomenological and microscopic models, such as the fission model [40], the cluster model [41], generalized liquid drop model [42], and the unified model for alpha decay and alpha capture [43], are available to study the different decay modes of superheavy nuclei. In addition, many studies have been concerned with the alpha decay and spontaneous fission of superheavy nuclei [44–46]. Simple empirical formulas are also available for determining the decay half-lives [47]. The possible isotopes of new superheavy elements are identified by studying the competition between different probable decay modes, such as α-decay, β-decay, cluster decay, and spontaneous fission. This study focuses on the different decay modes of superheavy nuclei in the atomic number range $104 \leq Z \leq 126$. After a detailed investigation of the competition between different decay modes, the possible isotopes and their decay modes with branching ratios are identified in the superheavy nuclei region. Hence, the contribution of this study is in the prediction of the most possible decay mode in superheavy nuclei, and in the identification of possible emitters in this superheavy region. The formalism is explained in Sect. 2. The analysis of different decay modes and possible emitters in the superheavy region is explained in Sect. 2.4. The paper is concluded in Sect. 3.

2 Theory

2.1 Alpha decay and cluster decay

In the effective liquid-drop model (ELDM), the α-decay half-life is computed using the relation

$$T_{1/2}(s) = \frac{\ln 2}{\nu_0 P P_\alpha}, \tag{1}$$

where ν_0 is the assault frequency on the barrier, and $\nu_0 = 1.8 \times 10^{22} s^{-1}$ [48]. P_α is the preformation factor, which is closely related to the shell structure [49]. The empirical formula for P_α is expressed as

$$\begin{aligned} \log P_\alpha = {} & p_1 + p_2(Z - Z_1)(Z_2 - Z) \\ & + p_3(N - N_1)(N_2 - N) + p_4 A, \end{aligned} \tag{2}$$

where N, Z, and A are the neutron, charge, and mass number of the parent nucleus, respectively, Z_1 and Z_2 are

the proton magic numbers around Z ($Z_1 \leq Z \leq Z_2$), and N_1 and N_2 are the neutron magic numbers around N ($N_1 \leq N \leq N_2$). p_1, p_2, and p_3 correspond to parameters in the region even(Z)-even(N), even(Z)-odd(N), odd(Z)-even(N), and odd(Z)-odd(N). They are presented in Table I of Ref. [50]. P is the Gamow penetrability factor, given by the expression

$$P = \exp\left[-\frac{2}{\hbar}\int_{\zeta_0}^{\zeta_c}\sqrt{2\mu[V(\zeta)-Q]}\mathrm{d}\zeta\right], \tag{3}$$

where μ is the inertial coefficient resulting from the Werner–Wheeler approximation [51]. The limits of integration ζ_0 and ζ_c are the inner and outer turning points, expressed as $\zeta_0 = R_\mathrm{p}$-$\bar{R_1}$ and $\zeta_c = \frac{Z_1 Z_2 e^2}{Q}$. R_p is the radius of the parent nucleus, and $\bar{R_1}$ is the final radius of the emitted cluster. In the ELDM, the total potential has been demonstrated to be the sum of Coulomb, proximity, and centrifugal potential [52, 53]. Hence, we can use the effective one-dimensional total potential energy as follows:

$$V = V_\mathrm{c} + V_\mathrm{s} + V_\ell. \tag{4}$$

To evaluate the Coulomb contribution in terms of the deformation parameter, we used V_c as defined in Ref. [54]:

$$V_\mathrm{c}(R) = \frac{e^2 Z_1 Z_2}{R} + 3Z_1 Z_2 e^2 \sum_{\lambda,i=1,2} \times \frac{R_i^\lambda(\alpha_i, T)}{(2\lambda+1)} Y_\lambda^{(0)}(\theta_i)\left[\beta_{\lambda i} + \frac{4}{7}\beta_{\lambda i}^2 Y_\lambda^{(0)}(\theta_i)\right], \tag{5}$$

with

$$R_i(\alpha_i) = R_{oi}\left[1 + \sum_\lambda \beta_{\lambda i} Y_\lambda^{(0)}(\alpha_i)\right], \tag{6}$$

where β_{λ_i} is the deformation parameter, $Y_{\lambda^{(0)}}$ are the spherical harmonics, and $R_{oi} = 1.28A_i^{1/3} - 0.76 + 0.8A_i^{-1/3}$. The effective surface potential can be calculated by

$$V_\mathrm{s} = \sigma_\mathrm{eff}(S_1 + S_2), \tag{7}$$

where S_1 and S_2 are the surface areas of the spherical fragments. σ_eff is the effective surface tension, which is defined as

$$\sigma_\mathrm{eff} = \frac{1}{4(R^2 - R_1^2 - R_2^2)}\left(Q - \frac{3}{20\pi\epsilon_0}e^2\left[\frac{Z^2}{R} - \frac{Z_1^2}{R_1} - \frac{Z_2^2}{R_2}\right]\right), \tag{8}$$

where R_2 is the final radius of the daughter fragment. The centrifugal potential energy is determined by

$$V_\ell = \frac{\hbar^2\ell(\ell+1)}{2\mu\zeta^2}, \tag{9}$$

where ℓ is the angular momentum of the emitted alpha/cluster and is calculated using the selection rules. In the case of alpha/cluster decay [55, 56], the selection rules follow the condition

$$|J_\mathrm{p} - J_\mathrm{d}| \leq \ell_\alpha \leq |J_\mathrm{p} + J_\mathrm{d}| \quad \text{and} \quad \frac{\pi_\mathrm{p}}{\pi_\mathrm{d}} = (-1)^{\ell_a}, \tag{10}$$

where $J_\mathrm{p}, \pi_\mathrm{p}$ and $J_\mathrm{d}, \pi_\mathrm{d}$ are the spin and parity of the parent and daughter nuclei, respectively. $\mu = \frac{M_1 M_2}{M_1 + M_2}$ is the reduced mass of the fragments, where M_1 and M_2 denote their atomic masses.

In ELDM, a system with two intersecting spherical nuclei with different radii is considered [52]. A schematic diagram for the representation of four independent coordinates, namely R_1, R_2, ζ, and ξ, is shown in Fig. 1. Three constraints are used to reduce the four-dimensional spherical problem to an equivalent one-dimensional problem. The geometric constraint given below is introduced so that the spherical segments remain in contact:

$$R_1{}^2 - (\zeta - \xi)^2 = R^2 - \xi^2. \tag{11}$$

The variables ζ and ξ represent the distance between the geometrical centers and the distance between the center of the heavier fragment and the circular sharp neck of the radius, respectively [53, 57]. Assuming that nuclear matter is incompressible, the constraint for the conservation of the total volume of the system is

$$2(R_1{}^3 + R_2{}^3) + 3[R_1{}^2(\zeta - \xi) + R_2{}^2\xi] - [(\zeta - \xi)^2 + \xi^3] = 4R^3, \tag{12}$$

where $R = r_0 A^{1/3}$ is the radius of the parent nucleus ($r_0 = 1.34$ fm is an adjustable parameter), with A being the mass number of the parent.

The radius of the α particle, R_1, is assumed to be constant in the varying mass asymmetry shape description:

$$R_1 - \bar{R_1} = 0, \tag{13}$$

where $\bar{R_1} = \left(\frac{Z_i}{Z}\right)^{1/3} R$, $i = 1, 2$; $\bar{R_1}$ provides the final radius of the α particle. Here, Z_1, Z_2, and Z are the atomic numbers of the α particle, daughter nucleus, and parent nucleus, respectively.

2.2 Beta decay

For all types of β processes, the expression for the half-life T_β is given by [58]

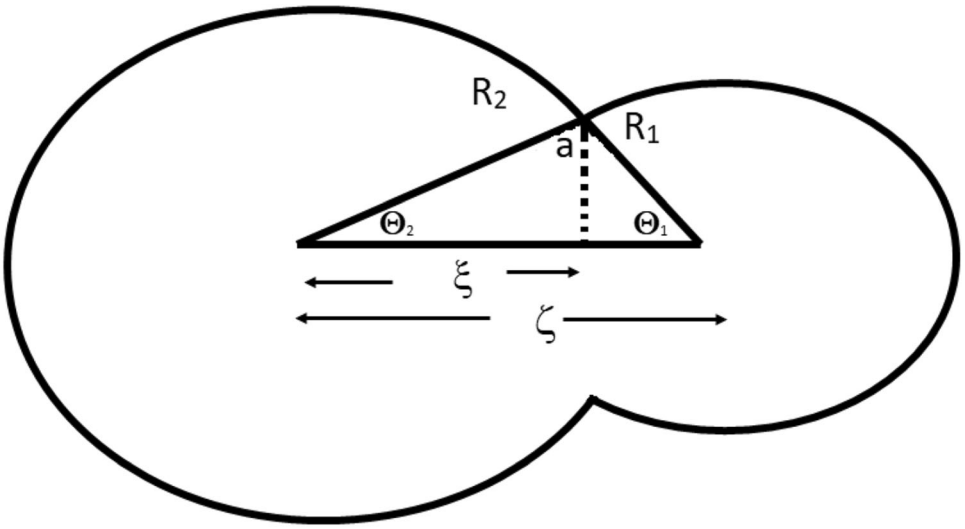

Fig. 1 Schematic presentation of molecular phase of the di-nuclear system (the daughter nucleus and the emitted (smaller) fragments). The distance between their geometrical centers and the distance between the center of the heavier fragment and the circular sharp neck of radius a are denoted by ζ and ξ, respectively

$$\frac{1}{T_\beta} = \frac{1}{T_{\beta^+}} + \frac{1}{T_{\beta^-}} + \frac{1}{EC}. \tag{14}$$

Here, EC is the electron capture. For a particular type of β-decay, the half-life is expressed as follows:

$$f_0{}^b T_b = \ln 2 \left[\frac{g^2 m_e{}^5 c^4}{2\pi^3 \hbar^7} |M_{if}|^2 \right]^{-1}. \tag{15}$$

Here, f_0^b is the Fermi function, $b = \beta^\pm$ or EC, m_e is the mass of the electron, and M_{if} is the transition matrix element between the initial and final states. The right-hand side of the above may be approximated by a constant for each type of β-decay [59]. This constant is different for allowed and forbidden cases of beta decay. For allowed β-decay, this constant has been determined as 5.7 ± 1.1 [60]. Equation (15) is reduced to

$$\log_{10}[f_0^b T_b(\text{sec})] = 5.7 \pm 1.1, \tag{16}$$

$$\log_{10}[f_0^b T_b] = 4.7. \tag{17}$$

2.2.1 $\beta^\pm$ decay

The Fermi function for β-decay is expressed as

$$f_0^\beta \pm = \int_1^{E_0} F(E,Z) P(E) (E_0 - E)^2 \mathrm{d}E. \tag{18}$$

Here, $P(E)$ is the momentum of the particle, and $F(E, Z)$ can be computed at the nuclear surface using the magnitude of the radial electron/positron wave function. The first approximation of $F(E, Z)$ is

$$F_0(E,Z) = \frac{2(\gamma+1)(2pR)^{2(\gamma-1)} \exp\left[\frac{\pi\xi}{p}\right] |\Gamma(\gamma + i\frac{\varepsilon}{p})|^2}{\Gamma^2(2\gamma+1)}. \tag{19}$$

Here, $\gamma = \sqrt{1-\alpha^2 Z^2}$, $\xi = \pm\, \alpha Z E$ (+ for β^- decay and − for β^+ decay), $\alpha = 1/137$ is the fine structure constant, R is the radius of the nucleus, and Γ is the gamma function.

At the surface of the nucleus (for β^+ decay), the orbital electron screening effect has a significant impact on the β electron/positron wave function. Thus, $F(E, Z)$ becomes

$$F(E,Z) = F_0(E \mp V_0, Z)^{\mp} (E \mp V_0, Z) \frac{p(E \mp V_0)(E \mp V_0)}{p(E)E}. \tag{20}$$

Here, $V_0 = 1.81\alpha^2 Z^{4/3}$, is the finite wavelength of the β particle, $p(E) = \sqrt{E^2 - 1}$ is the momentum of the β particle, $E_0 = 1 + Q_{\beta^\pm}/m_e c^2$ is the total limit energy of the β decay, $E = 1 + \varepsilon/m_e c^2$, and ε is the kinetic energy of the β particle

The expression for the energy released in β^+ decay is

$$Q_{\beta^+} = M(A,Z) - M(A,Z-1) - 2m_e c^2. \tag{21}$$

Similarly, for β^- decay,

$$Q_{\beta^-} = M(A,Z) - M(A,Z-1). \tag{22}$$

2.2.2 Electron capture

The value of Q for electron capture is given by

$$\begin{aligned} Q_{EC} &= M(A,Z) - M(A,Z-1) - B_e \\ &= Q_{\beta^+} + 2m_e c^2 - B_e. \end{aligned} \tag{23}$$

Here, B_e is the electron binding energy. Hence, even for the forbidden β^+ decay, electron capture is allowed. The capture of electrons of the K-shell for lower Z, and of the L-shell for higher Z is the major contributor to electron

capture. The contributions of the electrons of higher shells are negligible. Thus, the Fermi function becomes

$$f_0^{\mathrm{EC}} = f_0^K + f_0^{LI} + f_0^{LII}. \tag{24}$$

In general, for any shell,

$$f_0^X = \frac{\pi}{2}[E(Q_{\mathrm{EC}}) + E_X]^2[g_X^2(Z_X) + f_X^2(Z_X)] \quad X = K, L_{\mathrm{I}}, L_{\mathrm{II}}. \tag{25}$$

Here, E_X is the total energy of the electron:

$$E_K = \gamma, E_L = \left(\frac{1+\gamma}{2}\right)^{1/2}, \tag{26}$$

where Z_X is the effective charge, which considers the screening of the Coulomb field of the nucleus by other electrons [61]:

$$Z_K = Z - 0.35 \quad \text{and} \quad Z_L = Z - 4.15. \tag{27}$$

The nonzero components of the radial parts $(g_X \& f_X)$ of the wave function of the relativistic electron of orbit X are

Table 1 Cluster-decay half-lives obtained from present study (PS) and available experiments (exp)

Decay	Q_{Exp}(MeV)	$\log T_{1/2}^{\mathrm{exp}}$ [71]	$\log T_{1/2}^{\mathrm{PS}}$
^{221}Fr→ ^{14}C+^{207}Tl	31.317	14.51	14.91
^{221}Ra→^{14}C+^{207}Pb	32.396	13.37	13.56
^{222}Ra→^{14}C+^{208}Pb	33.05	11.05	12.70
^{223}Ra→^{14}C+^{209}Pb	31.829	15.05	13.94
^{224}Ra→^{14}C+^{210}Pb	30.54	15.9	15.52
^{226}Ra→^{14}C+^{212}Pb	28.2	21.29	22.74
^{225}Ac→^{14}C+^{211}Bi	30.477	17.16	17.06
^{228}Th→^{20}O+^{208}Pb	44.72	20.73	22.04
^{230}U→^{22}Ne+^{208}Pb	61.4	19.56	20.21
^{230}Th→^{24}Ne+^{206}Hg	57.571	24.61	25.07
^{231}Pa→^{24}Ne+^{207}Tl	60.417	22.89	23.07
^{232}U→^{24}Ne+^{208}Pb	62.31	20.39	22.25
^{233}U→^{24}Ne+^{209}Pb	60.486	24.84	25.05
^{234}U→^{26}Ne+^{208}Pb	59.466	25.93	25.62
^{234}U→^{28}Mg+^{206}Hg	74.11	25.74	26.04
^{236}Pu→^{28}Mg+^{208}Pb	79.67	21.65	22.07
^{238}Pu→^{28}Mg+^{210}Pb	75.912	25.66	25.98
^{238}Pu→^{30}Mg+^{208}Pb	77	25.66	26.25
^{238}Pu→^{32}Si+^{206}Hg	91.19	25.3	26.05
^{242}Cm→^{34}Si+^{208}Pb	96.509	23.11	24.24

Table 2 Comparison of logarithm half-lives (years) of spontaneous fission in the superheavy region $104 \le Z \le 114$ from present study with those from available experiments

Parent nuclei	$\log_{\mathrm{SF}}^{\mathrm{Expt}}$yr [72]	$\log_{\mathrm{SF}}^{\mathrm{Th}}$ yr
^{254}Rf	− 12.1	− 10.91
^{256}Rf	− 9.71	− 8.48
^{258}Rf	− 9.35	− 7.06
^{260}Rf	− 9.2	− 6.35
^{262}Rf	− 7.18	− 6.36
^{258}Sg	− 10	− 11.33
^{260}Sg	− 9.65	− 10.17
^{262}Sg	− 9.32	− 8.722
^{264}Sg	− 8.93	− 7.98
^{266}Sg	− 7.86	− 7.96
^{264}Hs	− 10.2	− 11.02
^{270}Ds	− 8.6	− 9.46
^{282}Cn	− 10.6	− 9.39
^{284}Cn	− 8.5	− 7.98
^{286}Fl	− 8.08	− 7.58

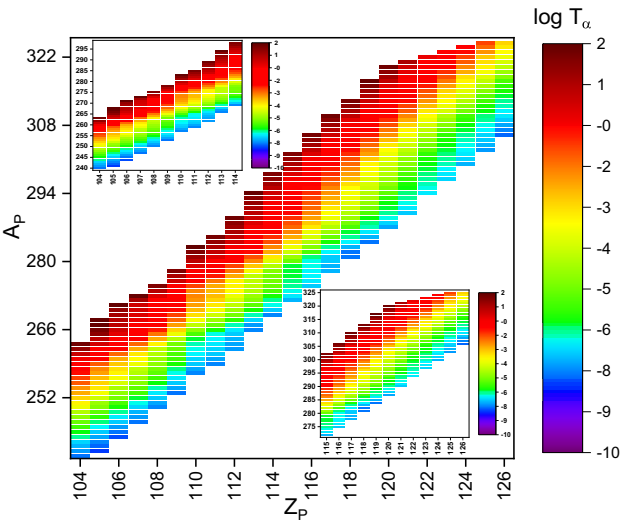

Fig. 2 (Color online) Map of nuclei reflecting the logarithmic α-decay half-lives for the isotopes of elements from $Z = 104$ to 126. The Q-values were estimated using AME16 and FRDM95. The vertical line on the right side of the figure shows an increase in the $\log T_{1/2}$ values from the navy-blue region to the brown region

$$g_K^2(Z) = \frac{4(1+\gamma)(2\alpha ZR)^{2(\gamma-1)}(\alpha Z)^3}{\Gamma(2\gamma+1)}, \tag{28}$$

Table 3 Comparison of alpha-decay half-lives from the present study (PS) and those from available experimental (Exp) values

Parent nuclei	Q_α (MeV)	$\log T_{1/2}$ (Exp)	$\log T_{1/2}$ (PS)
^{261}Bh	8.649	1.515	1.86
^{260}Db	9.379	− 0.295	0.11
^{269}Sg	8.8	2.27	2.12
^{265}Sg	9.078	0.869	1.15
^{263}Sg	9.391	− 0.932	0.12
^{261}Sg	9.803	− 1.469	− 1.21
^{272}Bh	9.3	1.025	0.78
^{271}Bh	9.5	0.176	0.18
^{270}Bh	9.3	1.785	1.02
^{277}Hs	8.4	− 2.523	− 1.02
^{273}Hs	9.9	− 0.119	− 0.32
^{269}Hs	9.629	0.851	0.65
^{274}Hs	9.5	0.079	0.21
^{278}Mt	9.1	0.653	1.65
^{276}Mt	9.8	− 0.284	0.05
^{274}Mt	10.5	− 0.357	− 0.98
^{281}Ds	8.958	1.104	1.45
^{282}Rg	9.38	2	1.85
^{280}Rg	9.98	0.623	0.55
^{279}Rg	10.45	− 1.046	− 1.04
^{285}Cn	8.793	1.447	2.85
^{283}Cn	9.62	0.623	0.89
^{281}Cn	10.28	− 0.886	− 0.68
^{284}Cn	9.301	1.013	1.78
^{277}Cn	11.622	− 2.551	− 2.65
^{286}Nh	9.68	0.978	1.22
^{285}Nh	10.02	0.623	0.76
^{284}Nh	10.25	− 0.013	0.08
^{283}Nh	10.6	− 1.125	− 0.98
^{289}Fl	9.847	0.279	0.96
^{288}Fl	9.969	− 0.18	− 0.16
^{287}Fl	10.436	− 0.319	− 0.28
^{286}Fl	10.7	− 0.921	− 0.87
^{285}Fl	11	− 0.824	− 1.89
^{290}Mc	10.3	− 0.187	0.18
^{289}Mc	10.6	− 0.481	− 0.35
^{293}Lv	8.886	− 1.244	0.12
^{292}Lv	10.707	− 1.886	− 0.96
^{291}Lv	11	− 1.721	− 1.45
^{289}Lv	11.7	− 2.848	− 2.97
^{294}Ts	8.963	− 1.292	0.06
^{294}Og	8.47	− 3.161	− 2.45
^{295}Og	9.056	− 1.745	0.58
^{298}120	13.355	− 3.051	− 4.68
^{299}120	13.105	− 3.15	− 1.58

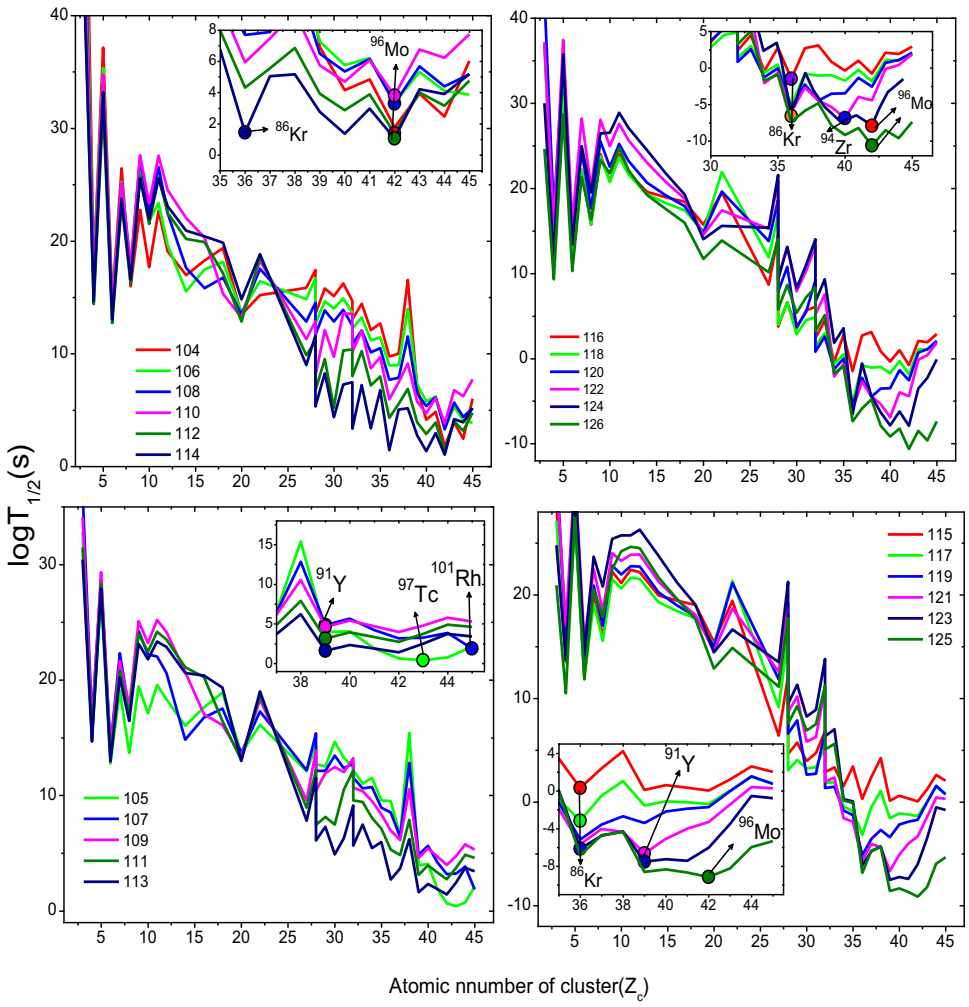

Fig. 3 (Color online) Predicted cluster-decay logarithmic half-lives in the atomic number range $Z = 104$–126 using AME16 and FRDM95 mass excess values. The hallow bin with different color in each panel shows the cluster emission corresponding to minimum half-lives

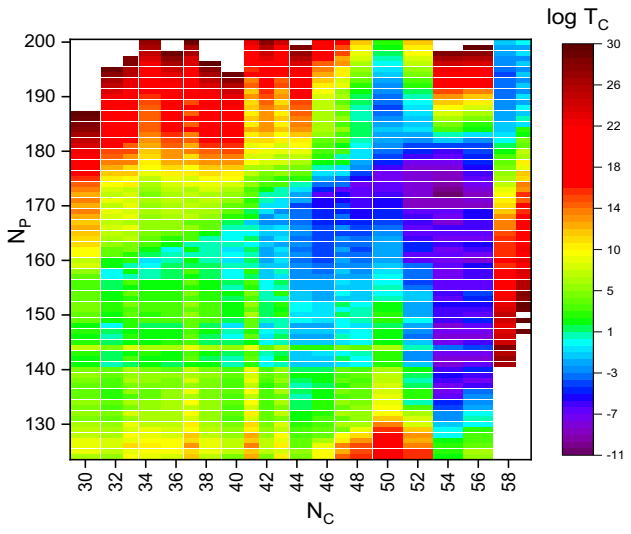

Fig. 4 (Color online) Map of nuclei reflecting the logarithmic cluster-decay half-lives for neutron number of parent and cluster isotopes of elements with $Z = 104$–126

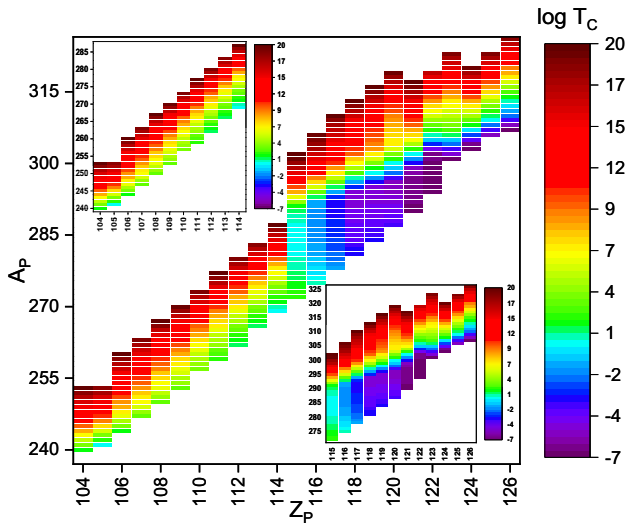

Fig. 5 (Color online) Heat map showing the variations of lowest logarithmic half lives of clusters with $104 < Z < 126$

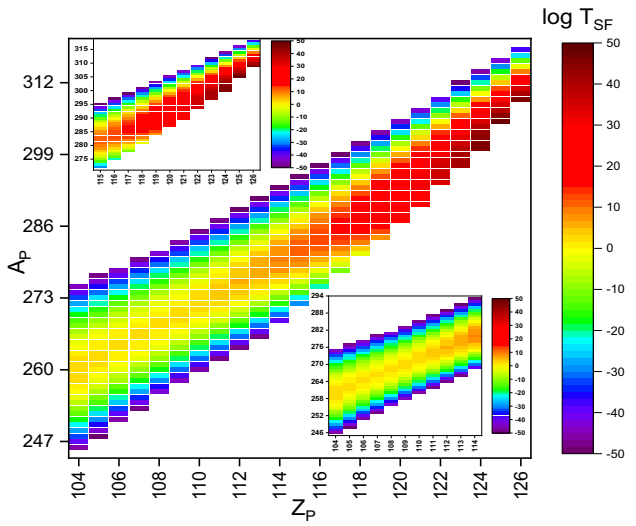

Fig. 6 (Color online) Heat map of the variations of logarithmic half-lives for spontaneous fission for $104 < Z < 126$

$$g_{LI}^2(Z) = \frac{[(2\gamma+2)^{1/2}+2](2\gamma+1)(2\alpha ZR)^{2(\gamma-1)}(\alpha Z)^3}{\Gamma(2\gamma+1)[(2\gamma+2)^{1/2}+1](2\gamma+2)^{\gamma}}, \tag{29}$$

$$g_{LII}^2(Z) = \frac{3}{16}(\alpha Z)^2 g_{LI}^2(Z). \tag{30}$$

2.3 Spontaneous fission

Spontaneous fission decay is studied by employing the quantum tunneling effect through the potential barrier. The decay constant of spontaneous fission is expressed as

$$\lambda = \frac{\ln 2}{T_{\mathrm{sf}}} = \nu S P_{\mathrm{S}}, \tag{31}$$

where ν, S, and P_{S} are model-dependent quantities, namely assault frequency, preformation probability, and barrier penetrability, respectively. In the above equation, $P = SP_{\mathrm{S}}$ and the spontaneous-fission half-lives are calculated as

$$T = \frac{\ln 2}{\nu P} = \frac{h \ln 2}{2} \frac{1}{E_\nu P}, \tag{32}$$

where h is the Planck constant, and $E_\nu = h\nu/2$ is the zero-point vibration energy. The penetration probability is evaluated using the action integral K:

$$P = \exp(-K), \tag{33}$$

and hence, the decimal logarithm of $T(s)$ is given by

$$\log_{10} T = 0.43429K - 20.8436 - \log_{10} E_\nu. \tag{34}$$

If $E_\nu = 0.5$ MeV, then the above equation becomes

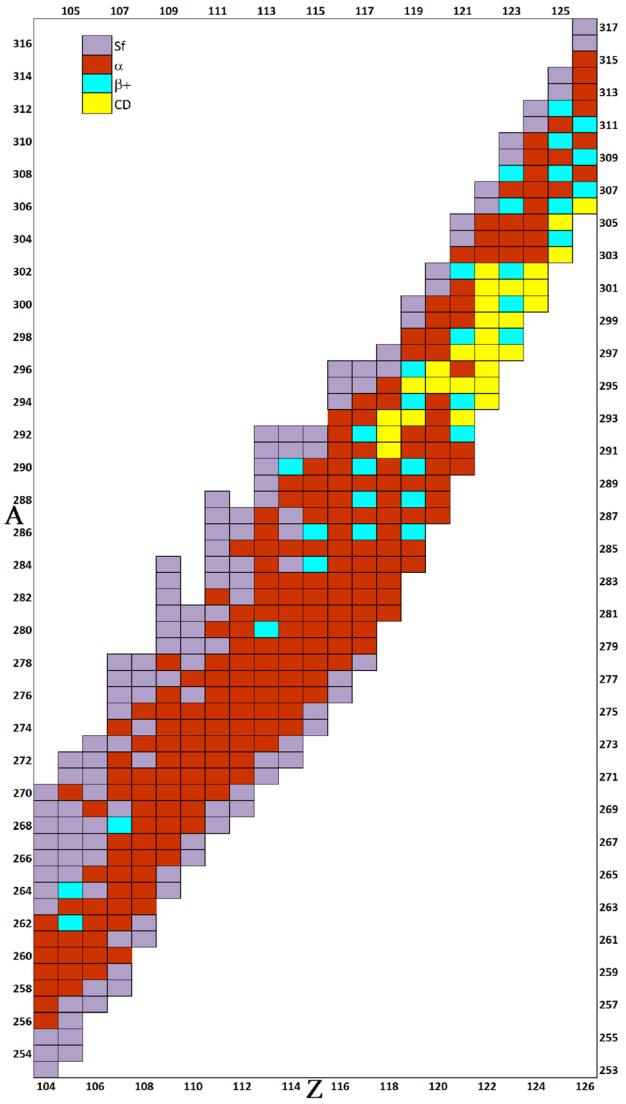

Fig. 7 (Color online) Chart of spontaneous fission (purple), alpha decay (brown), β^+-decay (cyan), and cluster emitters (yellow) with atomic numbers $Z = 104$–126. The Q-values were calculated using the FRDM95 mass tables

Table 4 Identified cluster emitters in the superheavy nuclei region

Parent nuclei	Q (MeV)	$\log T_{1/2}$	Cluster
^{292}Og	304.08	− 5.08	^{86}Kr
^{293}Og	303.63	− 4.63	^{86}Kr
^{298}122	338.25	− 6.02	^{94}Zr
^{300}122	337.45	− 6.21	^{94}Zr
^{299}123	338.66	− 7.18	^{91}Y
^{300}124	356.06	− 7.35	^{96}Mo
^{306}126	364.27	− 8.78	^{96}Mo

Table 5 Identified alpha emitters in the superheavy nuclei region

Parent nuclei	Q (MeV)	$\log T_{1/2}$	Parent nuclei	Q (MeV)	$\log T_{1/2}$	Parent nuclei	Q (MeV)	$\log T_{1/2}$
^{256}Rf	10.15	0.92	^{277}Ds	10.34	− 2.51	^{280}Lv	13.59	− 6.78
^{257}Rf	10.05	0.78	^{271}Rg	11.61	− 3.72	^{281}Lv	13.35	− 6.98
^{258}Rf	9.94	− 0.16	^{273}Rg	11.44	− 3.56	^{282}Lv	13.13	− 5.14
^{259}Rf	9.67	0.35	^{275}Rg	11.37	− 3.42	^{283}Lv	12.91	− 5.78
^{260}Rf	9.4	− 1.12	^{277}Rg	10.88	− 2.21	^{284}Lv	12.7	− 3.89
^{261}Rf	9.14	1.56	^{279}Rg	10.44	− 1.23	^{285}Lv	12.51	− 3.99
^{262}Rf	8.92	0.52	^{280}Rg	10.24	0.62	^{286}Lv	12.34	− 4.25
^{258}Db	10.45	0.55	^{282}Rg	9.89	2.15	^{287}Lv	12.19	− 3.98
^{259}Db	10.36	− 0.35	^{271}Cn	12.1	− 4.89	^{288}Lv	12.06	− 3.56
^{260}Db	10.08	0.26	^{272}Cn	11.96	− 4.65	^{290}Lv	11.83	− 1.75
^{261}Db	9.81	0.65	^{273}Cn	11.87	− 4.33	^{291}Lv	11.73	− 2.36
^{263}Db	9.34	1.52	^{274}Cn	11.8	− 4.16	^{292}Lv	11.64	− 1.88
^{270}Db	8.45	3.25	^{275}Cn	11.76	− 3.98	^{293}Lv	11.55	− 1.23
^{259}Sg	10.84	− 0.15	^{276}Cn	11.74	− 2.98	^{279}Ts	14.06	− 7.36
^{260}Sg	10.74	− 2.16	^{277}Cn	11.49	− 3.15	^{281}Ts	14.02	− 8.25
^{261}Sg	10.47	− 0.48	^{278}Cn	11.25	− 2.47	^{283}Ts	13.56	− 5.36
^{262}Sg	10.2	− 1.86	^{279}Cn	11.03	− 2.36	^{285}Ts	13.14	− 5.12
^{263}Sg	9.95	0.25	^{280}Cn	10.81	− 1.78	^{287}Ts	12.78	− 4.88
^{269}Sg	9.16	2.56	^{281}Cn	10.62	− 0.99	^{289}Ts	12.5	− 4.65
^{260}Bh	11.21	− 1.42	^{285}Cn	10	1.56	^{291}Ts	12.28	− 2.98
^{263}Bh	10.59	− 1.76	^{273}Nh	12.4	− 5.65	^{294}Ts	12	− 1.45
^{265}Bh	10.12	0.12	^{275}Nh	12.24	− 4.79	^{281}Og	14.44	− 7.65
^{266}Bh	9.94	0.22	^{276}Nh	12.2	− 4.78	^{282}Og	14.43	− 7.63
^{270}Bh	9.56	1.89	^{277}Nh	12.18	− 4.52	^{283}Og	14.19	− 7.45
^{271}Bh	9.53	0.18	^{279}Nh	11.7	− 2.89	^{284}Og	13.97	− 6.25
^{272}Bh	9.27	1.12	^{281}Nh	11.26	− 2.12	^{285}Og	13.76	− 6.41
^{274}Bh	8.78	1.23	^{282}Nh	11.07	− 1.69	^{286}Og	13.56	− 6.24
^{263}Hs	11.27	− 2.56	^{284}Nh	10.73	− 0.16	^{287}Og	13.37	− 5.25
^{265}Hs	10.77	− 4.56	^{285}Nh	10.59	0.78	^{288}Og	13.21	− 5.98
^{266}Hs	10.55	− 1.85	^{286}Nh	10.47	0.88	^{294}Og	12.53	− 3.88
^{267}Hs	10.37	− 1.42	^{287}Nh	10.35	0.76	^{295}Og	12.44	− 1.25
^{268}Hs	10.23	0.69	^{275}Fl	12.78	− 4.69	^{285}119	14.37	− 5.69
^{269}Hs	10.13	1.42	^{276}Fl	12.72	− 5.12	^{287}119	13.96	− 4.25
^{270}Hs	10.05	1.78	^{277}Fl	12.68	− 5.36	^{289}119	13.62	− 5.97
^{271}Hs	10	0.45	^{278}Fl	12.66	− 5.46	^{292}119	13.23	− 5.28
^{273}Hs	9.71	− 0.56	^{279}Fl	12.42	− 4.12	^{297}119	12.78	− 3.97
^{275}Hs	9.23	− 0.15	^{280}Fl	12.19	− 4.36	^{287}120	14.56	− 6.58
^{266}Mt	11.27	− 1.93	^{281}Fl	11.96	− 3.78	^{288}120	14.37	− 6.25
^{267}Mt	11.06	− 2.52	^{282}Fl	11.76	− 3.15	^{290}120	14.03	− 6.46
^{269}Mt	10.74	− 2.32	^{283}Fl	11.56	− 2.99	^{292}120	13.76	− 5.85
^{271}Mt	10.57	− 1.85	^{288}Fl	10.86	− 0.25	^{298}120	13.2	− 3.87
^{273}Mt	10.49	− 1.23	^{289}Fl	10.75	0.62	^{299}120	13.11	− 4.12
^{274}Mt	10.23	− 0.12	^{277}Mc	13.19	− 6.85	^{300}120	13.02	− 4.36
^{275}Mt	9.99	− 1.25	^{278}Mc	13.16	− 6.48	^{290}121	14.59	− 6.28
^{276}Mt	9.75	− 0.36	^{279}Mc	13.14	− 5.96	^{296}121	13.87	− 5.48
^{278}Mt	9.33	1.36	^{280}Mc	12.9	− 5.12	^{300}121	13.53	− 5.22

Table 5 continued

Parent nuclei	Q (MeV)	$\log T_{1/2}$	Parent nuclei	Q (MeV)	$\log T_{1/2}$	Parent nuclei	Q (MeV)	$\log T_{1/2}$
^{268}Ds	11.62	− 3.56	^{281}Mc	12.67	− 5.36	^{303}122	13.77	− 4.98
^{269}Ds	11.45	− 3.24	^{283}Mc	12.24	− 4.25	^{304}122	13.67	− 4.99
^{270}Ds	11.31	− 3.68	^{285}Mc	11.88	− 3.12	^{304}123	14.18	− 5.12
^{271}Ds	11.21	− 0.58	^{288}Mc	11.47	− 0.89	^{306}124	14.49	− 5.66
^{272}Ds	11.14	− 3.09	^{289}Mc	11.36	− 0.52	^{308}124	14.28	− 5.98
^{273}Ds	11.1	− 2.96	^{290}Mc	11.26	− 0.25	^{310}124	14.05	− 5.87
^{274}Ds	11.07	− 2.45	^{278}Lv	13.64	− 6.75			
^{275}Ds	10.81	− 2.12	^{279}Lv	13.61	− 6.12			

$\log_{10} T = -\log_{10} P - 20.5426$. The action integral K is evaluated as follows:

$$K = \frac{2\sqrt{2m}}{\hbar}\int_{R_a}^{R_b}(B(r)[E(R)-Q])^{1/2}\mathrm{d}R. \tag{35}$$

The term $E(R)$ is the macroscopic energy in terms of the surface, volume, Coulomb, proximity energy, shell correction, and pairing energy term [62], and m is the rest mass of the neutron. A few superheavies are spherical, the rest are deformed, primarily prolate or oblate. To include this effect, deformations are also involved in the calculation of $E(r)$, which is adopted from Ref. [62]. In the above equation, R is the separation distance between the center of the fission fragments, and R_a and R_b are the turning points, which are evaluated using the boundary conditions $E(R_a)$ and $E(R_b) = Q$. However, the term $B(r)$ is the inertia with respect to r and is evaluated using the semi-empirical model for inertia [63]:

$$B(r) = \mu\left(1 + k\exp\left[-\frac{128}{51}(r - R_{\mathrm{sph}}/R_0)\right]\right), \tag{36}$$

where μ and k are the reduced mass of the fission fragments and a semi-empirical constant ($k = 14.8$), respectively. R_{sph} is the distance between the center of mass of the fission fragments, set as $R_{\mathrm{sph}}/R_0 = 0.75$ in the symmetric case. The decay constant (λ) and the total fission decay constant are evaluated as described in Ref. [62].

2.4 Results and discussion

The mass excess values play a major role in the prediction of the decay mode and the corresponding half-lives. The predicted half-lives are sensitive to the Q-values, and small changes in the Q-values result in a notable change in the half-lives, with a magnitude of order 10^1 to 10^2 [36]. Mass excess tables such as WS4 [64], EBW [65], HFB28 and HFB29 [66], DZ10 [67], KTUY [68], finite-range droplet model (FRDM) [69], and AME16 [70] are available in the literature. In the present study, we used the updated AME16 [70] mass excess values up to $Z = 118$, and above $Z > 118$, the mass excess values are taken from the FRDM [69]. The dominant decay mode is identified by studying the competition between different decay modes: α-decay, β-decay, cluster decay, and spontaneous fission in the superheavy nuclei region $104 \leq Z \leq 126$.

A detailed literature review indicates that there is no experimental evidence for cluster radioactivity in the superheavy region. Furthermore, experimental studies of cluster decay in the actinide region are available. To validate the present study, the cluster-decay half-lives obtained

Table 6 Identified β^+ emitters in the superheavy nuclei region

Parent nuclei	Q (MeV)	$\log T_{1/2}$
^{264}Db	2.24	− 0.04
^{268}Bh	2.93	− 0.83
^{290}Fl	0.79	1.28
^{286}Mc	4.53	− 3.68
^{292}Ts	4.96	− 4.12
^{290}119	7.20	− 6.27
^{296}119	5.75	− 5.01
^{292}121	8.29	− 7.56
^{294}121	8.06	− 7.15
^{298}121	6.83	− 6.32
^{302}121	5.12	− 5.49
^{298}123	8.42	− 8.04
^{300}123	8.27	− 7.64
^{302}123	6.72	− 7.23
^{306}123	5.73	− 6.42
^{304}125	7.81	− 8.55
^{306}125	7.61	− 8.15
^{308}125	6.99	− 7.75
^{310}125	6.47	− 7.35
^{312}125	5.79	− 6.96

Table 7 Superheavy nuclei with dual decay mode and branching ratio

Parent nuclei	$\log T_{1/2}$				Decay mode		Parent nuclei	$\log T_{1/2}$				Decay mode	
	Sf	α	β^+	*CD*				*Sf*	α	β^+	*CD*		
^{263}Rf	1.25	1.98	1.65	36.6	$Sf = 57\%$	$\beta^+ = 43\%$	^{296}120	19.58	− 4.87	− 4.38	− 5.45	$CD = 53\%$	$\alpha = 47\%$
^{262}Db	2.31	− 0.48	− 0.51	34.76	$\beta^+ = 52\%$	$\alpha = 48\%$	^{291}120	25.45	− 6.21	− 5.85	− 4.69	$\alpha = 51\%$	$\beta^+ = 49\%$
^{264}Bh	0.71	− 1.65	− 1.75	20.58	$\beta^+ = 51\%$	$\alpha = 49\%$	^{297}120	15.36	− 4.25	− 4.6	− 3.62	$\beta^+ = 52\%$	$\alpha = 48\%$
^{262}Bh	− 3.25	− 3.25	− 2.22	17.73	$Sf = 50\%$	$Sf = 50\%$	^{289}120	21.36	− 6.31	− 6.27	− 4.3	$\alpha = 50\%$	$\beta^+ = 50\%$
^{266}Bh	1.62	− 1.89	− 1.29	23.6	$\alpha = 59\%$	$\beta^+ = 41\%$	^{293}120	25.32	− 5.18	− 5.43	− 5.06	$\beta^+ = 51\%$	$\alpha = 49\%$
^{264}Hs	− 2.98	− 3.15	− 1.11	15.37	$\alpha = 51\%$	$Sf = 49\%$	^{293}121	29.32	− 6.98	− 6.29	− 6.47	$\alpha = 52\%$	$CD = 48\%$
^{270}Mt	2.11	− 2.45	− 2.08	19.43	$\alpha = 54\%$	$\beta^+ = 46\%$	^{299}121	18.56	− 4.75	− 5.05	− 5.43	$CD = 52\%$	$\beta^+ = 48\%$
^{272}Mt	1.35	− 1.65	− 1.63	22.66	$\alpha = 50\%$	$\beta^+ = 50\%$	^{303}121	− 4.36	− 3.52	− 4.22	2.35	$Sf = 51\%$	$\beta^+ = 49\%$
^{268}Mt	0.99	− 2.78	− 2.54	16.53	$\alpha = 52\%$	$\beta^+ = 48\%$	^{291}121	25.87	− 5.94	− 6.7	− 6.65	$\beta^+ = 50\%$	$CD = 50\%$
^{276}Ds	− 1.72	− 1.65	− 0.09	23.61	$Sf = 51\%$	$\alpha = 49\%$	^{295}121	30.36	− 5.78	− 5.88	− 6.34	$CD = 52\%$	$\beta^+ = 48\%$
^{272}Rg	2.22	− 3.15	− 3.34	12.55	$\beta^+ = 51\%$	$\alpha = 49\%$	^{297}121	26.9	− 4.77	− 5.46	− 6.33	$CD = 54\%$	$\beta^+ = 46\%$
^{276}Rg	2.42	− 2.16	− 2.44	18.44	$\beta^+ = 53\%$	$\alpha = 47\%$	^{301}121	8.25	− 5.36	− 4.64	− 1.47	$\alpha = 54\%$	$\beta^+ = 46\%$
^{269}Rg	− 3.98	− 3.86	− 2.95	9.04	$Sf = 51\%$	$\alpha = 49\%$	^{294}122	30.65	− 5.98	− 6.51	− 6.89	$CD = 51\%$	$\beta^+ = 49\%$
^{270}Rg	− 1.56	− 3.87	− 3.79	10.12	$\alpha = 51\%$	$\beta^+ = 49\%$	^{295}122	34.25	− 5.99	− 6.73	− 6.78	$CD = 50\%$	$\beta^+ = 50\%$
^{278}Rg	− 1.32	− 1.54	− 1.99	21.54	$\beta^+ = 56\%$	$\alpha = 44\%$	^{296}122	36.89	− 6.24	− 6.1	− 6.83	$CD = 52\%$	$\alpha = 48\%$
^{274}Rg	3.56	− 3.22	− 2.89	15.4	$\alpha = 53\%$	$\beta^+ = 47\%$	^{297}122	34.22	− 6.96	− 6.32	− 6.77	$\alpha = 51\%$	$CD = 49\%$
^{283}Nh	− 1.55	− 1.89	− 1.55	18.55	$\alpha = 55\%$	$Sf = 45\%$	^{305}122	− 0.58	− 4.98	− 4.68	− 0.68	$\alpha = 52\%$	$\beta^+ = 48\%$
^{274}Nh	0.65	− 4.01	− 4.6	6.88	$\beta^+ = 53\%$	$\alpha = 47\%$	^{302}122	18.21	− 5.27	− 4.87	− 6.31	$CD = 54\%$	$\alpha = 46\%$
^{280}Nh	4.98	− 2.78	− 3.27	14.3	$\beta^+ = 54\%$	$\alpha = 46\%$	^{301}122	23.56	− 5.96	− 5.5	− 6.46	$CD = 52\%$	$\alpha = 48\%$
^{278}Nh	5.88	− 3.87	− 3.72	11.51	$\alpha = 51\%$	$\beta^+ = 49\%$	^{299}122	30.89	− 6.14	− 5.91	− 6.7	$CD = 52\%$	$\alpha = 48\%$
^{274}Fl	− 5.12	− 4.89	− 3.95	3.62	$Sf = 51\%$	$\alpha = 49\%$	^{303}122	13.77	− 5.11	− 5.09	− 4.33	$\alpha = 50\%$	$\beta^+ = 50\%$
^{285}Fl	− 0.45	− 2.11	− 1.97	16.71	$\alpha = 52\%$	$\beta^+ = 48\%$	^{303}123	27.89	− 6.36	− 5.96	− 3.66	$\alpha = 52\%$	$\beta^+ = 48\%$
^{282}Mc	11.02	− 3.78	− 4.55	0.52	$\beta^+ = 55\%$	$\alpha = 45\%$	^{297}123	38.48	− 6.17	− 7.18	− 7.51	$CD = 51\%$	$\beta^+ = 49\%$
^{287}Mc	1.32	− 2.98	− 2.4	0.5	$\alpha = 55\%$	$\beta^+ = 45\%$	^{301}123	35.02	− 6.18	− 6.37	− 6.86	$CD = 52\%$	$\beta^+ = 48\%$
^{284}Mc	8.98	− 3.58	− 4.12	0.37	$\beta^+ = 54\%$	$\alpha = 46\%$	^{307}123	2.18	− 4.98	− 5.15	2.81	$\beta^+ = 51\%$	$\alpha = 49\%$
^{276}Mc	− 3.12	− 5.89	− 5.86	1.45	$\alpha = 50\%$	$\beta^+ = 50\%$	^{305}123	15.58	− 5.48	− 5.56	− 0.65	$\beta^+ = 50\%$	$\alpha = 50\%$
^{277}Lv	− 6.85	− 5.78	− 5.42	0.18	$Sf = 54\%$	$\alpha = 46\%$	^{308}123	− 4.89	− 5.26	− 6.01	3.61	$\beta^+ = 53\%$	$\alpha = 47\%$
^{289}Lv	3.15	− 3.05	− 2.83	− 1.32	$\alpha = 52\%$	$\beta^+ = 48\%$	^{303}124	40.25	− 6.25	− 6.83	− 6.77	$\beta^+ = 50\%$	$CD = 50\%$
^{293}Ts	− 2.98	− 3.58	− 2.84	− 2.88	$\alpha = 55\%$	$Sf = 45\%$	^{305}124	33.21	− 5.12	− 6.42	− 4.29	$\beta^+ = 56\%$	$\alpha = 44\%$
^{284}Ts	13.25	− 5.25	− 5.83	− 2.5	$\beta^+ = 53\%$	$\alpha = 47\%$	^{302}124	40.25	− 5.96	− 6.6	− 7.13	$CD = 52\%$	$\beta^+ = 48\%$
^{286}Ts	14.55	− 5.16	− 5.4	− 2.6	$\beta^+ = 51\%$	$\alpha = 49\%$	^{304}124	35.85	− 6.01	− 6.19	− 6.45	$CD = 51\%$	$\beta^+ = 49\%$
^{290}Ts	9.18	− 4.36	− 4.55	− 3.09	$\beta^+ = 51\%$	$\alpha = 49\%$	^{307}124	22.14	− 5.97	− 6.02	− 0.09	$\beta^+ = 50\%$	$\alpha = 50\%$

Table 7 continued

Parent nuclei	$\log T_{1/2}$				Decay mode		Parent nuclei	$\log T_{1/2}$				Decay mode	
	Sf	α	β^+	*CD*				*Sf*	α	β^+	*CD*		
^{288}Ts	13.78	− 4.87	− 4.98	− 2.91	$\beta^+ = 51\%$	$\alpha = 49\%$	^{301}124	44.14	− 6.04	− 7.23	− 7.53	$CD = 51\%$	$\beta^+ = 49\%$
^{280}Ts	0.68	− 6.25	− 6.69	− 2.01	$\beta^+ = 52\%$	$\alpha = 48\%$	^{309}124	6.87	− 5.11	− 5.62	3.17	$\beta^+ = 52\%$	$\alpha = 48\%$
^{282}Ts	8.58	− 5.85	− 6.26	− 2.19	$\beta^+ = 52\%$	$\alpha = 48\%$	^{309}125	26.25	− 6.51	− 6.49	0.26	$\alpha = 50\%$	$\beta^+ = 50\%$
^{290}Og	16.98	− 3.78	− 3.91	− 4.72	$CD = 55\%$	$\beta^+ = 45\%$	^{307}125	38.21	− 6.21	− 6.89	− 3.75	$\beta^+ = 53\%$	$\alpha = 47\%$
^{291}Og	14.89	− 3.78	− 4.13	− 4.9	$CD = 54\%$	$\beta^+ = 46\%$	^{311}125	11.58	− 5.75	− 6.09	2.43	$\beta^+ = 51\%$	$\alpha = 49\%$
^{289}Og	18.74	− 5.25	− 4.56	− 4.46	$\alpha = 54\%$	$\beta^+ = 46\%$	^{305}125	45.35	− 6.87	− 7.29	− 7.5	$CD = 51\%$	$\beta^+ = 49\%$
^{284}119	5.95	− 6.68	− 7.53	− 3.17	$\beta^+ = 53\%$	$\alpha = 47\%$	^{303}125	45.25	− 6.96	− 7.69	− 8.07	$CD = 51\%$	$\beta^+ = 49\%$
^{293}119	18.29	− 3.98	− 4.57	− 5.15	$CD = 53\%$	$\beta^+ = 47\%$	^{315}126	− 1.58	− 5.75	− 6.17	2.82	$\beta^+ = 52\%$	$\alpha = 48\%$
^{286}119	14.98	− 7.25	− 7.11	− 3.79	$\alpha = 50\%$	$\beta^+ = 50\%$	^{313}126	15.25	− 6.24	− 6.57	0.85	$\beta^+ = 51\%$	$\alpha = 49\%$
^{294}119	15.98	− 3.89	− 5.43	− 5.15	$\beta^+ = 51\%$	$CD = 49\%$	^{308}126	48.21	− 6.87	− 7.12	− 5.37	$\beta^+ = 51\%$	$\alpha = 49\%$
^{288}119	19.35	− 5.85	− 6.69	− 4.15	$\beta^+ = 53\%$	$\alpha = 47\%$	^{311}126	32.21	− 5.12	− 6.96	− 0.97	$\beta^+ = 58\%$	$\alpha = 42\%$
^{298}119	− 4.85	− 3.22	− 4.59	0.23	$Sf = 51\%$	$\beta^+ = 49\%$	^{310}126	39.21	− − 6.32	− 6.73	− 1.99	$\beta^+ = 52\%$	$\alpha = 48\%$
^{291}119	21.25	− 4.58	− 4.99	− 4.74	$\beta^+ = 51\%$	$CD = 49\%$	^{309}126	44.58	− 6.58	− 7.36	− 3.69	$\beta^+ = 53\%$	$\alpha = 47\%$
^{295}119	11.35	− 4.23	− 4.15	− 5.03	$CD = 54\%$	$\alpha = 46\%$	^{312}126	26.12	− 5.74	− 6.33	0.01	$\beta^+ = 52\%$	$\alpha = 48\%$
^{295}120	22.15	− 4.78	− 5.02	− 5.46	$CD = 52\%$	$\beta^+ = 48\%$	^{307}126	51.32	− 7.11	− 7.75	− 6.99	$\beta^+ = 52\%$	$\alpha = 48\%$
^{294}120	23.58	− 4.22	− 4.79	− 5.36	$CD = 53\%$	$\beta^+ = 47\%$	^{314}126	7.56	− 6.21	− 5.94	1.7	$\alpha = 51\%$	$\beta^+ = 49\%$

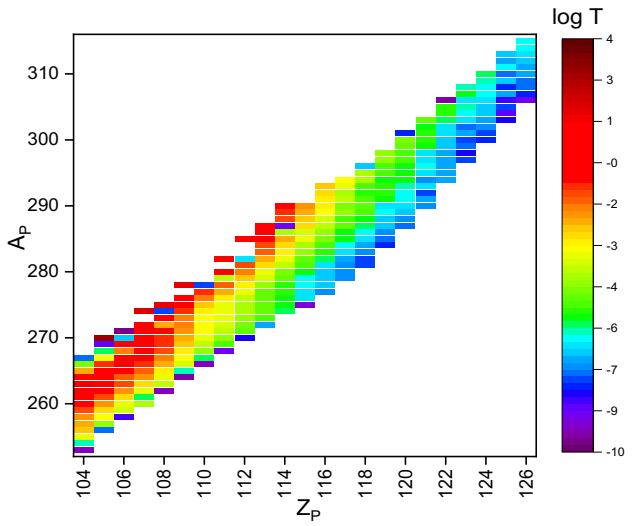

Fig. 8 (Color online) Heat map showing the variations of atomic number, mass number of parent and logarithmic half-lives of different decay modes (life times) for $104 < Z < 126$

in the present study in the actinide region were compared with the experiments, and good agreement was observed. With this confidence, we studied cluster decay in the superheavy region, and the results are presented in Table 1. Similarly, Table 2 shows a comparison of the studied logarithmic half-lives (in years) of spontaneous fission from the present study with those from available experiments. It can be seen that the cluster-decay and spontaneous-fission half-lives obtained in the present study are close to those of the experiments.

As a part of this investigation, we studied the α-decay properties of superheavy nuclei using the formalism explained in the theory section. The predicted alpha-decay half-lives were validated by comparison with those from available experiments in the superheavy region. The results are given in Table 3.

From the comparison, it is observed that the predicted half-lives are in good agreement with those of the experiments. With this confidence, we obtained the alpha-decay half-lives of superheavy nuclei in the region $104 \leq Z \leq 126$ Fig. 2.

shows a wide range of α-decay half-lives. For a given superheavy nucleus, the alpha decay half-lives increase as the neutron number of its isotopes increases. For instance, the α-decay half-lives are of the order of nanoseconds at $N/Z = 1.307692$ for Rutherfordium, whereas for the same superheavy element, the α-decay half-lives are of the order of 10^2s at $N/Z = 1.504762$. Similarly, all neutron-rich superheavy nuclei have comparably longer α-decay half-lives, which is in agreement with the report available in Ref. [73]. The obtained α-decay half-lives of all possible superheavy nuclei are presented in the heat map in Fig. 2. The right vertical bar shows the magnitude of the $\log T_{1/2}$ values. The color variation from navy blue to wine indicates values in the range 10^{-10}–10^2 s. The contrast in the blue region lies between 10^{-10} s and 10^{-7} s, in the green region, it lies in the range 10^{-6}–10^{-4} s, and the range $10^{-4} - 10^{-3}$ s is presented in the yellow region. Finally, the red-to-wine region shows higher half-lives in the range $10^{-2} - 10^2$ s. The inset of Fig. 2 on the top left side provides information on the magnified portion of α-decay half-lives in the superheavy region $Z = 104 - 114$, whereas the bottom-right inset provides information on the magnified portion of the superheavy region $Z = 115 - 126$. After the detailed investigation of the α-decay, a search was made to identify the cluster emitters in the superheavy region. Cluster radioactivity is energetically favorable if the Q-values are positive. We studied the possibility of cluster decay with $3 \leq Z_c \leq 45$ in the superheavy region $104 \leq Z \leq 126$. For a given parent nucleus, the half-lives corresponding to various cluster emission were evaluated, and the cluster corresponding to shorter half-lives was identified. Furthermore, the cluster emitters corresponding to shorter half-lives for different isotopes of a given superheavy element were also identified. Eventually, cluster emissions corresponding to the shortest half-lives T_c were identified; these are referred to as cluster-decay half-lives (T_c). The predicted cluster decay half-lives in the atomic number region $104 \leq Z \leq 126$ correspond to all the studied cluster emissions, as shown in Fig. 3.

This figure enables us to identify the cluster emission corresponding to the shorter half-lives of a given superheavy element. The half-lives of superheavy nuclei with $Z = 115$–120 against cluster radioactivity are shorter for ^{86}Kr than those of the other studied clusters. The superheavy nuclei with $Z = 104$, 106, 108, 110, 112, 114, 124, and 126 have shorter half-lives against ^{96}Mo cluster emissions than those of the other studied clusters. The decay half-lives are shorter for the ^{91}Y emission from superheavy nuclei with $Z = 109$, 111, 113, 121, and 123. Similarly, the half-lives of superheavy nuclei with $Z = 105$ and 107 against cluster radioactivity are shorter for ^{97}Tc and ^{101}Rh than those of the other studied clusters.

Cluster radioactivity in the superheavy nuclei region has shorter half-lives for cluster neutron numbers 44–48 from parent nuclei with neutron numbers 130–200, as shown in Fig. 4.

The range of cluster decay half-lives for superheavy elements with $104 \leq Z \leq 126$ is shown in Fig. 5.

Shorter half-lives are observed for $N/Z > 1.37068$, and larger half-lives are observed for $N/Z < 1.37068$. From the figure, it is clear that up to superheavy nuclei $104 \leq Z \leq 115$, larger cluster-decay half-lives are observed, whereas shorter cluster-decay half-lives are observed in the

superheavy region $116 \leq Z \leq 126$. The inset of Fig. 5 on the top-left side shows a magnified portion of the logarithmic half-lives (T_c) in the superheavy region $104 \leq Z \leq 115$, whereas the inset at the right bottom shows a magnified portion of the shorter logarithmic half-lives (T_c) in the superheavy region $116 \leq Z \leq 126$. This figure also shows that some of the superheavy nuclei have lifetimes of the order of ns to μs and exhibit cluster decay.

The other prominent decay mode that was studied is spontaneous fission, which is also energetically feasible in heavy and superheavy nuclei. It may occur in such nuclei owing to an increase in the Coulomb interactions. References [10, 11, 38, 74–77] report consistent α-decay chains from superheavy nuclei followed by spontaneous fission. The spontaneous fission half-lives are studied using the theory explained in Sect. 2.3. The variations of spontaneous fission half-lives in the superheavy region $Z = 104$–126 are shown in Fig. 6.

The $\log T_{SF}$ values vary between -50(dark blue region) and 50 (dark-red region). For instance, at atomic number $Z = 104$, for isotopes 245–275, the $\log T_{1/2}$(SF) values ranging from -50 to 5 are shown, whereas the half-lives with smaller values are indicated by the color range from navy blue to blue. The half-lives ranging from nanoseconds to 10^5 s are indicated by the color range from yellow to light orange. Similarly, in the atomic number range $Z = 119$ and above, larger values of spontaneous-fission logarithmic half-lives are indicated by the red color range. Thus, on either side of Fig. 6, for isotopes corresponding to the atomic number range $Z = 104$–126, smaller half-lives are observed, whereas in the middle region of the figure, larger values of $\log T_{1/2}$ are observed up to $Z = 116$. In contrast, smaller half-lives are observed for higher isotopes ($Z > 116$), and larger $\log T_{1/2}$ for lower isotopes ($Z < 116$). A similar trend was also observed in a previous study [78], in which the half-lives of nuclei $Z = 92$–104 were compared with experimentally available values.

A detailed investigation of the Q-values corresponding to β-decay in the superheavy region demonstrates that β^+-decay is energetically possible with $Z = 105$, 107, 113, 114, 115, 117, 119, 121, 123, 125, and 126, whereas β^--decay is not energetically possible. Furthermore, we also studied β-decay half-lives using the formalism explained in Sect. 2.2.1.

The competition between different possible decay modes, namely α-decay, cluster-decay, β-decay and spontaneous fission, enables us to identify the dominant decay mode for superheavy elements in the atomic number region $104 \leq Z \leq 126$ of all possible isotopes Fig. 7.

shows the decay modes of the superheavy nuclei. In the studied superheavy region, we identified around 20 β^+emitters, which are presented in Table 6. We also identified 35 cluster emitters, which are presented in Table 4.

It was demonstrated that the majority of superheavy nuclei undergo α-decay and spontaneous fission. The α-emitting superheavy nuclei are listed in Table 5.

The identified alpha emitters have half-lives of approximately μs to 100 s in the superheavy region $104 \leq Z \leq 126$. Table 4 lists the identified cluster emissions with the corresponding half-lives. The amount of energy released during cluster emission, cluster emitted, and $\log T_{1/2}$ values are presented in the table. The minimum cluster decay half-lives correspond to ^{86}Kr, ^{94}Zr, ^{91}Y, and ^{96}Mo for the nuclei $^{292-293}$Og, ^{298,300}122, ^{299}123, ^{300}124, and ^{306}126, respectively. From the available literature, it is also evident that the heavy particle radioactivity of ^{86}Kr is observed in the superheavy nucleus $Z = 118$ [36, 79]. In addition, Rb, Sr, Y, Zr, Nb, and Mo cluster emissions [80] were observed for $Z = 119$–124, respectively. As in previous studies, in the present study, shorter half-lives in the superheavy region $Z = 118$, 122-124, and 126 were observed, with ^{86}Kr, ^{94}Zr, ^{91}Y, and ^{96}Mo cluster emissions, respectively. Similarly, approximately 20 possible β^+ emitters were identified in the superheavy region $105 \leq Z \leq 125$, and they are presented in Table 6.

The information provided Table 7 regarding the half-lives and branching ratios presents ambiguities in terms of determining a single decay mode. The branching ratios relative to the minimum half-lives among the studied decay modes are obtained, and the second column of the table shows the $\log T_{1/2}$ values corresponding to spontaneous-fission, α-decay, β^+-decay, and cluster-decay half-lives. For instance, the superheavy nucleus ^{263}Rf exhibits shorter $\log T_{1/2}$ values for spontaneous fission and β^+-decay than for other decay modes. The branching ratio of spontaneous fission and β^+-decay was obtained, and it was found that the branching ratio corresponding to spontaneous fission and β^+ was 55% and 45%, respectively. Similarly, we identified the branching ratios for the superheavy region $104 \leq Z \leq 126$, which are presented in Table 7.

Finally, Fig. 8 shows the lifetimes of the superheavy elements after the competition between different decay modes was studied.

It can be seen that the lifetime varies from ns to min and decreases as the atomic number increases. For instance, the average lifetime of a superheavy element with $Z = 104$ is approximately 10 min, whereas that of a hypothetical superheavy element with $Z = 126$ is of the order of ms.

3 Conclusion

We systematically investigated all possible decay modes, namely α-decay, β-decay, cluster decay, and spontaneous fission, in the superheavy region $104 \leq Z \leq 126$. The findings of this study were validated by comparison with experiments. Approximately 20 β^+ and 7 heavy particle emitters were found in the superheavy region. Furthermore, the nuclei with almost the same half-lives for the two decay modes were also reported, with the corresponding branching ratios. However, an experimental study is necessary to draw definite conclusions.

Author contributions All authors contributed to the study conception and design. Conceived of the original idea, developed the theory formulation of work and writing by HCM and NS. Performed the computations and performed, analytic calculations and graphical representation by PSDG, KNS and AMN, data analysis by LS and SACR. All authors read and approved the final manuscript.

References

1. F.P. Hebberger, S. Hofmann, D. Ackermann et al., Decay properties of neutron-deficient isotopes 256,257 Db, 255 Rf, 252,253 Lr. Eur. Phys. J. A **12**, 57–67 (2001). https://doi.org/10.1007/s100500170039
2. Y.T. Oganessian, V.K. Utyonkov, Y.V. Lobanov et al., Publisher's note: Measurements of cross sections and decay properties of the isotopes of elements 112, 114, and 116 produced in the fusion reactions 233,238 U, 242 Pu, and 248 Cm + 48 Ca. Phys. Rev. C **70**, 064609 (2004). https://doi.org/10.1103/PhysRevC.71.029902
3. Y.T. Oganessian, V.K. Utyonkov, Y.V. Lobanov et al., Publisher's note: measurements of cross sections and decay properties of the isotopes of elements 112, 114, and 116 produced in the fusion reactions ^{233,238} U, ^{242} Pu, and ^{248} Cm + ^{48} Ca. Phys. Rev. C **71**, 029902 (2005). https://doi.org/10.1103/PhysRevC.71.029902
4. G.G. Adamian, N.V. Antonenko, W. Scheid, High-spin isomers in some of the heaviest nuclei: spectra, decays, and population. Phys. Rev. C **81**, 024320 (2010). https://doi.org/10.1103/PhysRevC.81.024320
5. A.T. Kruppa, M. Bender, W. Nazarewicz et al., Shell corrections of superheavy nuclei in selfconsistent calculations. Phys. Rev. C **61**, 034313 (2000). https://doi.org/10.1103/PhysRevC.61.034313
6. Y. Shi, D.E. Ward, B.G. Carlsson et al., Structure of superheavy nuclei along decay chains of element 115. Phys. Rev. C **90**, 014308 (2014). https://doi.org/10.1103/PhysRevC.90.014308
7. X. Meng, B. Lu, S. Zhou, Ground state properties and potential energy surfaces of ^{270}Hs from multidimensionally-constrained relativistic mean field model. Sci. China I Phys. Mech. Astron. **63**, 1–11 (2020). https://doi.org/10.1007/s11433-019-9422-1
8. R. Swain, B. Sahu, Structure and reaction dynamics of she $Z = 130$. Chin. Phys. C **43**, 104103 (2019). https://doi.org/10.1088/1674-1137/43/10/104103
9. F. Niu, P.-H. Chen, H.-G. Cheng et al., Multinucleon transfer dynamics in nearly symmetric nuclear reactions. Nucl. Sci. Tech. **31**, 59 (2020). https://doi.org/10.1007/s41365-020-00770-1
10. S. Hofmann, V. Ninov, F.P. Heberger et al., Production and decay of ^{269}110. Zeitschrift fur Physik A Hadrons and Nuclei **350**, 277–280 (1995). https://doi.org/10.1007/BF01291181
11. S. Hofmann, G. Munzenberg, The discovery of the heaviest elements. Rev. Mod. Phys. **72**, 733–767 (2000). https://doi.org/10.1103/RevModPhys.72.733
12. D. Boilley, B. Cauchois, H. Lv et al., How accurately can we predict synthesis cross sections of superheavy elements? Nucl. Sci. Tech. **29**, 172 (2018). https://doi.org/10.1007/s41365-018-0509-7
13. D. Naderi, S.A. Alavi, Influence of the shell effects on evaporation residue cross section of superheavy nuclei. Nucl. Sci. Tech. **29**, 161 (2018). https://doi.org/10.1007/s41365-018-0498-6
14. X. Li, Z. Wu, L. Guo, Entrancechannel dynamics in the reaction ^{40}Ca +^{208}Pb. Sci. China-Phys. Mech. Astron. **62**, 12 (2019). https://doi.org/10.1007/s11433-019-9435-x
15. Y.T. Oganessian, K.P. Rykaczewski, A beachhead on the island of stability. Phys. Today (2015). https://doi.org/10.1063/PT.3.2880
16. A. Sobiczewski, F.A. Gareev, B.N. Kalinkin, Closed shells for $Z > 82$ and $N > 126$ in a diffuse potential well. Phys. Lett. **22**, 500–502 (1966). https://doi.org/10.1016/0031-9163(66)91243-1
17. S. Nilsson, Binding states of individual nucleons in strongly deformed nuclei. Dan. Mat. Fys. Med. **29**, 1–69 (1955)
18. M. Bender, K. Bennaceur, T. Duguet et al., Tensor part of the skyrme energy density functional: ii: deformation properties of magic and semimagic nuclei. Phys. Rev. C **80**, 064302 (2009). https://doi.org/10.1103/PhysRevC.80.064302
19. B.A. Brown, The nuclear shell model towards the drip lines. Prog. Part. Nucl. Phys. **47**, 517–599 (2001). https://doi.org/10.1016/S0146-6410(01)00159-4
20. R.D. Herzberg, P.T. Greenlees, P.A. Butler et al., Nuclear isomers in superheavy elements as stepping stones towards the island of stability. Nature **442**, 896–899 (2006). https://doi.org/10.1038/nature05069
21. D. Tománek, M.A. Schlüter, Calculation of magic numbers and the stability of small si clusters. Phys. Rev. Lett. **56**, 1055–1058 (1986). https://doi.org/10.1103/PhysRevLett.56.1055
22. A.M. Nagaraja, H.C. Manjunatha, N. Sowmya et al., Cluster radioactivity in superheavy nuclei $^{299-302}$120. Indian J. Pure Appl. Phys. **58**, 207–212 (2020)
23. H.C. Manjunatha, N. Sowmya, Competition between spontaneous fission ternary fission cluster decay and alpha decay in the superheavy nuclei of $Z = 126$. Nucl. Phys. A **969**, 68–82 (2018). https://doi.org/10.1016/j.nuclphysa.2017.09.008
24. N. Sowmya, H.C. Manjunatha, N. Dhananjaya et al., Competition between binary fission, ternary fission, cluster radioactivity and alpha decay of ^{281}Ds. J. Radioanal. Nucl. Chem. **323**, 1347–1351 (2020). https://doi.org/10.1007/s10967-019-06706-3
25. G.R. Sridhar, H.C. Manjunatha, N. Sowmya et al., Atlas of cluster radioactivity in actinide nuclei. Eur. Phys. J. Plus **135**, 1–28 (2020). https://doi.org/10.1140/epjp/s13360-020-00302-1
26. H.C. Manjunatha, K.N. Sridhar, N. Sowmya, Investigations of the synthesis of the superheavy element $Z = 122$. Phys. Rev. C **98**, 024308 (2018). https://doi.org/10.1103/PhysRevC.98.024308
27. H.C. Manjunatha, N. Sowmya, Decay modes of superheavy nuclei $Z = 124$. Int. J. Mod. Phys. E **27**, 1850041 (2018). https://doi.org/10.1142/S0218301318500416
28. N. Sowmya, H.C. Manjunatha, Investigations on different decay modes of darmstadtium. Phys. Particles Nuclei Lett. **17**, 370–378 (2020). https://doi.org/10.1134/S1547477120030140
29. N. Sowmya, H.C. Manjunatha, Competition between different decay modes of superheavy element $Z = 116$ and synthesis of possible isotopes. Braz. J. Phys. **49**, 874–886 (2019). https://doi.org/10.1007/s13538-019-00710-4

30. N. Sowmya, H.C. Manjunatha, P.S.D. Gupta, Competition between decay modes of superheavy nuclei $^{281-310}$Og. Int. J. Mod. Phys. E (2020). https://doi.org/10.1142/S0218301320500871
31. N. Sowmya, H.C. Manjunatha, Investigations on the synthesis and decay properties of roentgenium. Braz. J. Phys. **50**, 317–330 (2020). https://doi.org/10.1007/s13538-020-00747-w
32. N. Sowmya, H.C. Manjunatha, P.S.D. Gupta et al., Competition between cluster and alpha decay in odd Z superheavy nuclei $111 \leq Z \leq 125$. Braz. J. Phys. **51**, 99–135 (2021). https://doi.org/10.1007/s13538-020-00801-7
33. K.N. Sridhar, H.C. Manjunatha, H.B. Ramalingam, Search for possible fusion reactions to synthesize the superheavy element $Z = 121$. Phys. Rev. C **98**, 064605 (2018). https://doi.org/10.1103/PhysRevC.98.064605
34. A. Soylu, Search for decay modes of heavy and superheavy nuclei. Chin. Phys. C **43**, 074102 (2019). https://doi.org/10.1088/1674-1137/43/7/074102
35. Nuclear live chart. https://www-nds.iaea.org/relnsd/vcharthtml/VChartHTML.html
36. D.N. Poenaru, R.A. Gherghescu, W. Greiner, Heavy-particle radioactivity of superheavy nuclei. Phys. Rev. Lett. **107**, 062503 (2011). https://doi.org/10.1103/PhysRevLett.107.062503
37. Y.T. Oganessian, Route to islands of stability of superheavy elements. Phys. Atom. Nuclei **63**, 1315–1336 (2000). https://doi.org/10.1134/1.1307456
38. Y. Oganessian, Heaviest nuclei from ^{48}Ca induced reactions. J. Phys. G **34**, R165 (2007). https://doi.org/10.1016/j.nuclphysa.2015.07.003
39. J. Grumann, U. Mosel, B. Fink et al., Investigation of the stability of superheavy nuclei around $Z = 114$ and $Z = 164$. Zeitschrift fur Physik **228**, 371–386 (1969). https://doi.org/10.1007/BF01406719
40. D.N. Poenaru, M. Ivaşcu, A. Sndulescu et al., Atomic nuclei decay modes by spontaneous emission of heavy ions. Phys. Rev. C **32**, 572–581 (1985). https://doi.org/10.1103/PhysRevC.32.572
41. B. Buck, A.C. Merchant, S.M. Perez, α decay calculations with a realistic potential. Phys. Rev. C **45**, 2247–2253 (1992). https://doi.org/10.1103/PhysRevC.45.2247
42. H.F. Zhang, G. Royer, Theoretical and experimental α decay half-lives of the heaviest odd-Z elements and general predictions. Phys. Rev. C **76**, 017304 (2007). https://doi.org/10.1103/PhysRevC.76.047304
43. V.Y. Denisov, H. Ikezoe, α-nucleus potential for α-decay and sub-barrier fusion. Phys. Rev. C **72**, 064613 (2005). https://doi.org/10.1103/PhysRevC.72.064613
44. P. Möller, G.A. Leander, J.R. Nix, On the stability of the transeinsteinium elements. Zeitschrift fr Physik A Atomic Nuclei **323**, 41–45 (1986). https://doi.org/10.1007/BF01294553
45. F.R. Xu, E.G. Zhao, R. Wyss et al., Enhanced stability of superheavy nuclei due to high-spin isomerism. Phys. Rev. Lett. **92**, 252501 (2004). https://doi.org/10.1103/PhysRevLett.92.252501
46. C. Wong, Additional evidence of stability of the superheavy element 310126 according to the shell model. Phys. Lett. **21**, 688–690 (1966). https://doi.org/10.1016/0031-9163(66)90127-2
47. D.N. Poenaru, R.A. Gherghescu, W. Greiner, Single universal curve for cluster radioactivities and α decay. Phys. Rev. C **83**, 014601 (2011). https://doi.org/10.1103/PhysRevC.83.014601
48. S.B. Duarte, F.G. Oap, T.A. Dimarco, Half-lives for proton emission, alpha decay, cluster radioactivity, and cold fission processes calculated in a unified theoretical framework. Atom. Data Nucl. Data Tables **80**, 235 (2002). https://doi.org/10.1006/adnd.2002.0881
49. H.F. Zhang, G. Royer, Y.J. Wang et al., Analytic expressions for α particle preformation in heavy nuclei. Phys. Rev. C **80**, 057301 (2009). https://doi.org/10.1103/PhysRevC.80.057301
50. Z. Shan, Z. Yanli, C. Jianpo et al., Improved semi-empirical relationship for α-decay half-lives. Phys. Rev. C **95**, 014311 (2017). https://doi.org/10.1103/PhysRevC.95.014311
51. D.N. Poenaru, J.A. Maruhn, W. Greiner et al., Inertia and fission paths in a wide range of mass asymmetry. Zeitschrift fur Physik A Atomic Nuclei **333**, 291 (1989). https://doi.org/10.1007/BF01294517
52. M. Gongalves, S.B. Duarte, Effective liquid drop description for the exotic decay of nuclei. Phys. Rev. C **48**, 2409–2414 (1993). https://doi.org/10.1103/PhysRevC.48.2409
53. M. Gonçalves, N. Teruya, O. Tavares et al., Twoproton emission half-lives in the effective liquid drop model. Phys. Lett. B **774**, 14–19 (2017). https://doi.org/10.1016/j.physletb.2017.09.032
54. K. Santhosh, R. Biju, Stability of ^{248,254}Cf isotopes against alpha and cluster radioactivity. Ann. Phys. **334**, 280–287 (2013). https://doi.org/10.1016/j.aop.2013.04.008
55. H.C. Manjunatha, G.R. Sridhar, N. Sowmya et al., A systematic study of alpha decay in actinide nuclei using modified generalized liquid drop model. Int. J. Mod. Phys. E **30**, 2150013 (2021). https://doi.org/10.1142/S0218301321500130
56. N. Maroufi, V. Dehghani, S.A. Alavi, Alpha and cluster decay of some deformed heavy and superheavy nuclei. Nucl. Phys. A **983**, 77–89 (2019). https://doi.org/10.1016/j.nuclphysa.2018.12.023
57. M. Gonçalves, S.B. Duarte, Effective liquid drop description for the exotic decay of nuclei. Phys. Rev. C **48**, 2409–2414 (1993). https://doi.org/10.1103/PhysRevC.48.2409
58. B.S. Dzhelepov, L.N. Zyryanova, Y.P. Suslov, Beta processes functions for the analysis of beta spectra and electron capture. **373**(1972)
59. A.V. Karpov, V.I. Zagrebaev, Y. MartinezPalenzuela et al., Decay properties and stability of heaviest elements. Int. J. Mod. Phys. E **21**, 1250013 (2012). https://doi.org/10.1142/S0218301312500139
60. C.S. Wu, S.A. Moszkowski, Beta decay. **183**(1966)
61. M. A. Preston. Addison-Wesley Publishing Company, Inc., (1962)
62. X. Bao, H. Zhang, G. Royer et al., Spontaneous fission half-lives of heavy and superheavy nuclei within a generalized liquid drop model. Nucl. Phys. A **906**, 1–13 (2013). https://doi.org/10.1016/j.nuclphysa.2013.03.002
63. J. Randrup, S.E. Larsson, P. Moller et al., Spontaneous-fission half-lives for even nuclei with $Z \geq 92$. Phys. Rev. C **13**, 229–239 (1976). https://doi.org/10.1103/PhysRevC.13.229
64. N. Wang, M. Liu, X. Wu et al., Surface diffuseness correction in global mass formula. Phys. Lett. B **734**, 215–219 (2014). https://doi.org/10.1016/j.physletb.2014.05.049
65. M.W. Kirson, Mutual influence of terms in a semi-empirical mass formula. Nucl. Phys. A **798**, 29–60 (2008). https://doi.org/10.1016/j.nuclphysa.2007.10.011
66. S. Goriely, Further explorations of skyrme-hartree- fock-bogoliubov mass formulas. XV. The spin-orbit coupling. Nucl. Phys. A **933**, 68–81 (2015). https://doi.org/10.1016/j.nuclphysa.2014.09.045
67. J. Duflo, A. Zuker, Microscopic mass formulas. Phys. Rev. C **52**, R23–R27 (1995). https://doi.org/10.1103/PhysRevC.52.R23
68. H. Koura, T. Tachibana, M. Uno et al., Nuclidic mass formula on a spherical basis with an improved even-odd term. Prog. Theor. Phys. **113**, 305–325 (2005). https://doi.org/10.1143/PTP.113.305
69. Reference input parameter library (ripl-3). https://www-nds.iaea.org/RIPL-3
70. M. Wang, G. Audi, F.G. Kondev et al., The ame2016 atomic mass evaluation (ii): tables, graphs and references. Chin. Phys. C

41, 030003 (2017). https://doi.org/10.1088/1674-1137/41/3/030003
71. K.P. Santhosh, R.K. Biju, A. Joseph, A semi-empirical model for alpha and cluster radioactivity. J. Phys. G **35**, 082102 (2008). https://doi.org/10.1088/0954-3899/35/8/085102
72. C. Xu, Z. Ren, Y. Guo, Competition between α decay and spontaneous fission for heavy and superheavy nuclei. Phys. Rev. C **78**, 044329 (2008). https://doi.org/10.1103/PhysRevC.78.044329
73. J.P. Wieleczko, E. Bonnet, J. Gomez del Campo et al., Influence of the n/z ratio on disintegration modes of compound nuclei. AIP Conf. Proc. **1098**, 64–69 (2009). https://doi.org/10.1063/1.3108862
74. Y.T. Oganessian, V.K. Utyonkov, Y.V. Lobanov et al., Synthesis of superheavy nuclei in the ^{48}Ca+^{244}Pu reaction: ^{288}114. Phys. Rev. C **62**, 041604 (2000). https://doi.org/10.1103/PhysRevC.62.041604
75. Y.T. Oganessian, V.K. Utyonkov, Y.V. Lobanov et al., Observation of the decay of ^{292}116. Phys. Rev. C **63**, 011301 (2000). https://doi.org/10.1103/PhysRevC.63.011301
76. Y.T. Oganessian, V.K. Utyonkov, Y.V. Lobanov et al., Measurements of cross sections for the fusion-evaporation reactions ^{244}Pu(^{48}Ca, xn)$^{292-x}$114 and ^{245}Cm(^{48}Ca, xn)$^{293-x}$116. Phys. Rev. C **69**, 054607 (2004). https://doi.org/10.1103/PhysRevC.69.054607
77. K. Morita, K. Morimoto, D. Kaji et al., Experiment on the synthesis of element 113 in the reaction ^{209}Bi(^{70}Zn, n) ^{278}113. J. Phys. Soc. Jpn. **73**, 2593–2596 (2004). https://doi.org/10.1143/JPSJ.73.2593
78. A. Baran, K. Pomorski, A. Lukasiak et al., A dynamic analysis of spontaneous-fission halflives. Nucl. Phys. A **361**, 83–101 (1981). https://doi.org/10.1016/0375-9474(81)90471-1
79. Z. Matheson, S.A. Giuliani, W. Nazarewicz et al., Cluster radioactivity of $^{294}_{118}$Og$_{176}$. Phys. Rev. C **99**, 041304 (2019). https://doi.org/10.1103/PhysRevC.99.041304
80. D.N. Poenaru, R.A. Gherghescu, W. Greiner, Heavy-particle radioactivity. J. Phys. Conf. Ser. (2013). https://doi.org/10.1088/1742-6596/436/1/012056